

A comparison of time domain electromagnetic and surface nuclear magnetic resonance sounding for subsurface water on Mars

Robert E. Grimm¹

Blackhawk Geoservices, Inc., Golden, Colorado, USA

Received 18 February 2002; revised 9 August 2002; accepted 28 February 2003; published 22 April 2003.

[1] The time domain electromagnetic (TDEM) method has enjoyed wide success in terrestrial groundwater exploration, and the contrast in electrical conductivity between dry overburden and groundwater containing even a small amount of dissolved solids on Mars will yield a robust response. However, moist clays or even ores (e.g., massive hematite) will also be electrically conductive and could be mistaken for aquifers on Mars if proper geologic context is lacking. Surface nuclear magnetic resonance (SNMR) is the only noninvasive geophysical method that responds nearly uniquely to water. As the measured EMF is proportional to the proton-precession frequency, which in turn is proportional to the planet's static magnetic field, SNMR signals are comparatively weak. Using small systems of several kilograms and several watts, the exploration depth of SNMR is one to two orders of magnitude smaller than TDEM: the latter can detect water to depths up to a few kilometers, whereas the former is limited to depths of a few tens of meters. There is no improvement in SNMR signal-to-noise with increasing static field where penetration is controlled by aquifer salinity (skin depth). As reasonable integration times cannot substantially increase the exploration depth, much larger transmitter current or loop mass (either requiring system masses of tens to hundreds of kilograms) are the only way to implement SNMR for exploration to depths of at least hundreds of meters. In spite of some ambiguity in target identification, TDEM is recommended for the first generation of in situ active-source EM measurements for groundwater on Mars. *INDEX TERMS:* 6225 Planetology: Solar System Objects: Mars; 5794 Planetology: Fluid Planets: Instruments and techniques; 0925 Exploration Geophysics: Magnetic and electrical methods; *KEYWORDS:* Mars, groundwater, electromagnetic sounding, time domain electromagnetics, nuclear magnetic resonance

Citation: Grimm, R. E., A comparison of time domain electromagnetic and surface nuclear magnetic resonance sounding for subsurface water on Mars, *J. Geophys. Res.*, 108(E4), 8037, doi:10.1029/2002JE001882, 2003.

1. Introduction

[2] The principal Mars exploration themes encompassing geology, climate, life, and preparation for human exploration all incorporate assessment of subsurface, liquid water as a key goal [*Mars Exploration Program/Payload Analysis Group (MEPAG)*, 2001]. The present-day surface temperature and estimated heat flux indicate that free liquid water will not be reached typically until depths of 2–7 km [*Clifford*, 1993]. However, the recently discovered “gullies,” apparently fluvial and geologically recent, suggest contemporary sources of liquid water at depths less than a few hundred meters [*Malin and Edgett*, 2000]. As shallow groundwater obviously will be the most practical drilling goal [see *Blacic et al.*, 2000], robust identification of any such sites will receive the highest exploration priority.

[3] The high-resolution, ground-penetrating radar selected for the 2005 Mars Reconnaissance Orbiter seeks to map the

upper few hundred meters of Mars and would therefore appear well matched to this search. However, radar is not the optimum tool for groundwater exploration on Earth; even in dry overburden on Mars, strong losses may occur due to scattering, magnetic absorption, and multiple reflections. Contrasts in permittivity or dielectric constant between water and rock or soil are still not large enough that water may always be identified unambiguously. Finally, the skin depth in aquifers with even modest amount of dissolved solids will severely limit radar penetration.

[4] Low-frequency electromagnetic (EM) methods, those that exploit induction rather than wave propagation, have dominated terrestrial groundwater exploration at depths of hundreds of meters (see *McNeill* [1990] for a review) for two reasons. First, low frequencies are able to penetrate to greater depths and these diffusive signals are less affected by small-scale geological heterogeneity than wave methods like radar or seismic. Second, low-frequency EM is sensitive to electrical conductivity instead of permittivity. Contrasts in the former range over many orders of magnitude and aquifers can be inferred when formations have relatively low conductivity (fresh water) or high conductivity (salt water) relative to their surroundings.

¹Also at Laboratory for Atmospheric and Space Physics, University of Colorado, Boulder, Colorado, USA.

[5] For Mars, groundwater that has not been in meteoric circulation for aeons (if ever) will likely be saline and therefore be a near-ideal low-frequency EM target. *Grimm* [2002] examined the ability of both natural-source and artificial-source EM soundings to detect and characterize groundwater on Mars as functions of aquifer depth, thickness, and salinity. If the appropriate ambient natural energy is absent, the time domain electromagnetic (TDEM) method was preferred for exploration to depths of hundreds of meters or more. However, EM methods can be so sensitive to water, as a humid clay or as supercooled thin films in the cryosphere, that it may be difficult to distinguish true aquifers from trace amounts of water. Furthermore, identification of water is still not totally unambiguous, as other electrically conductive formations, particularly those that are strataform, may be mistaken for aquifers. The hematite exposures of Sinus Meridiani [*Christensen et al.*, 2000] and the “stealth” region west of Tharsis [*Muhleman et al.*, 1991] may represent such materials if present at depth.

[6] Little or no ambiguity in detection of subsurface water exists for just one geophysical method: nuclear magnetic resonance (NMR). The bulk spins of hydrogen nuclei in water can be aligned with a static magnetic field and the abundance measured by perturbing those spins with a second, time-varying magnetic field. Solids and liquids can easily be separated using the recovery time to the perturbation, so groundwater can be distinguished from ice. Other hydrogen-containing compounds (such as hydrocarbons) can be assimilated in the water response, but even in terrestrial geophysical investigations this is neglected because the spectroscopic separation of these compounds requires very large magnetic fields that can be created only in the laboratory.

[7] NMR of course has been used in geophysics for decades, not to determine the proton abundance using a fixed magnetic field but to measure the magnetic field using a specified proton abundance: the proton magnetometer. The borehole NMR tool has become standard in the logging industry, providing not just estimates of free-fluid abundance but also the distribution of pore sizes and inferences of permeability. In order to image the subsurface using NMR from the surface (SNMR), the planet’s static magnetic field must be used as the reference field and a loop used to provide the time-varying perturbation. These factors have two key implications. First, the field operation, in which a transient pulse is generated and the signal recorded during transmitter off-time, is very similar to TDEM. Second, SNMR signals are orders of magnitude smaller than those in laboratory measurements or medical imaging because the voltage response is proportional to the static field (see below). This also implies that SNMR signals will be much smaller than TDEM for the same resources (loop size, transmitter power, integration time).

[8] The purpose of this paper is to compare TDEM and SNMR performance for detection of subsurface water on Mars and, in particular, to assess the relative merits of these methods using the same hardware deployed to the planet’s surface. The trade lies between the nearly unique assessment of water provided by SNMR but with a more limited depth of exploration than TDEM. Because a static magnetic field is required but near-surface fields are likely highly variable on Mars, the geographic coverage provided by

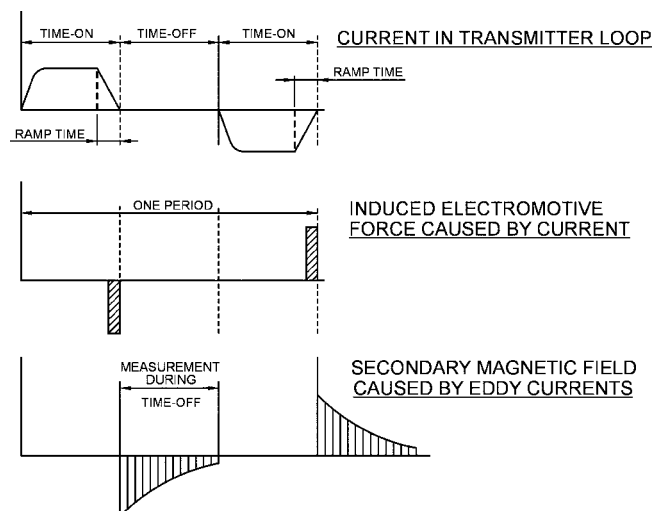


Figure 1. Time series for the time domain electromagnetic (TDEM) method (after *McNeill* [1990]). Bipolar waveform is used to eliminate DC drift, but note that t_T in text refers to time between pulses, regardless of polarity.

SNMR may be limited. The joint use of TDEM and NMR has been well recognized: the methods have been employed together for simultaneous delineation of aquifers and evaluation of water quality [*Goldman et al.*, 1994], and in very saline or clay-rich environments, the NMR inversion must be corrected by TDEM sounding or equivalent to include ground conductivity [*Shushakov*, 1996].

2. Time Domain Electromagnetics (TDEM)

[9] TDEM methods measure the transient inductive response of the subsurface to a step- or pulse-like transmitted waveform (see *McNeill* [1990], *Hoekstra and Blohm* [1990], and *Spies and Frischknecht* [1991] for reviews). A static magnetic field is established while the transmitter current is on, most commonly using a loop. When this field is changed, usually by abrupt extinction, the EMF generated according to Faraday’s Law causes eddy or secondary currents to flow in the ground (Figure 1). At the instant of transmitter turn-off, eddy currents reproduce the static magnetic field but then decay rapidly. These changing currents induce new currents in the ground at greater depth. Either the magnetic field or EMF induced by these secondary currents is recorded at the surface and inverted for the conductivity-depth profile or geoelectric section. Because measurements are made during transmitter off-time, results are insensitive to details of the loop layout. Measurements can be made using the same loop as transmitter and receiver (coincident-loop) or with a separate receiver. The latter is often placed in the middle of the transmitter loop and is therefore called central-loop. When the target is deep compared to the coil size, the results are insensitive to the relative positions of the coils. The coincident-loop arrangement is the simplest as it does not require a separate receiver; furthermore, signals can be large from the integrated flux over the large loop area. However, noise can also be large in this arrangement, particularly in ground with frequency-dependent permeability [e.g., *Spies and Frisch-*

knecht, 1991]. Laterites commonly form such “superparamagnetic” soils on Earth; given the significant oxidation at the surface of Mars, magnetic losses could severely degrade coincident-loop experiments. Because the effect is largest within a few meters of the transmitter wire, superparamagnetic signatures can usually be easily eliminated by separating transmitter and receiver. For the purposes of this paper (and because present commercial NMR equipment is coincident-loop; see below), two simple receiver configurations are considered: coincident-loop measuring EMF and central-loop measuring magnetic field.

[10] A simple model representing an aquifer as a thin conductive plate [Kaufman, 1994] can adequately represent the TDEM response of potential aquifers on Mars (see Grimm [2002] for detailed development). The plate is assumed to lie at a depth greater than a few loop diameters so that the transmitted field may be considered to be that of a dipole. Immediately after transmitter turn-off, the secondary vertical magnetic induction at the center of the transmitter loop is

$$B_z^{TDEM} = \mu M_T / 16\pi d^3 \quad (1)$$

and the EMF in the loop is

$$V^{TDEM} = 3\mu b M_T M_R / 32\pi d^4 \quad (2)$$

where μ is the permeability of free space, M_T is the transmitter moment, M_R is the receiver moment, d is the distance from the instrument to the aquifer, and $b = 2/\mu S$, where S is the plate’s conductance. The latter is given as $S = \sigma h$ where σ is the conductivity and h is the thickness. The receiver moment for a square loop is $M_R = nD^2$, where n is the number of turns and D is the loop diameter; for a coincident-loop sounding the transmitter moment is $M_T = IM_R$, where I is the current.

[11] Note that the magnetic field (or induction) on the plate at transmitter turn-off is a static image of the dipole primary, falling off as $1/d^3$ and is independent of the plate conductance. The magnetic field therefore provides a direct indicator of target depth. In contrast, the voltage falls off as $1/d^4$ and varies inversely with plate conductance: thicker or more conductive plates actually result in smaller signals immediately after transmitter turn-off. Although EMF measurements have been the general rule in TDEM, magnetic field measurements are actually superior for discrete targets such as the conductive plate. For both magnetic field and EMF the plate conductance can be determined by the rate of decay of the measured quantity [see Kaufman, 1994; Grimm, 2002]. Here only the signal at transmitter turn-off is calculated, with signal-to-noise ratio (SNR) specified to track the time decay through, say, an order of magnitude in amplitude.

[12] The maximum depth to which the conductive plate can be detected may be derived by solving equations (1) and (2) for d at a specified signal level in B_z or V . The detection threshold must incorporate the spectral noise density, the specified SNR, and the bandwidth reduction achieved by signal integration or stacking. Using the results of Becker and Cheng [1988], Grimm [2002] showed that the noise bandwidth for a TDEM system is approximately

$$v = 5/4t_0 f_T \Delta \quad (3)$$

where t_0 is the integration time, f_T is the transmitter pulse rate, and Δ is the receiver gate width.

[13] Grimm [2002] used equations (1)–(3) to demonstrate that a compact TDEM system, with masses of a few-to-several kilograms and consuming several watts of power, could robustly detect water on Mars to depths of at least several hundred meters. Here the critical parameters of loop size and integration time are explored in greater detail and in a way consistent with comparison to SNMR.

[14] A typical TDEM instrument such as the Geonics EM-47 (www.geonics.com) or the Zonge NanoTem (www.zonge.com) consists of transmitter and receiver units, batteries, a transmitter loop, and a receiver coil. A loop capable of carrying several amperes is typically 14 gauge, i.e., 1.6-mm diameter. The mass of the entire system is few tens of kilograms. One notable compact unit is the AEMR TEM-FAST (www.aemr.boom.ru) whose prototype was designed for Russian TDEM soundings on Mars (E. Fainberg, personal communication, 2000). The mass of the entire TEM-FAST system, including batteries, external computer, and the coincident transmitter/receiver loop, is 5 kg; the Mars-flight prototype was apparently lighter. Ozorovich *et al.* [1999] have continued investigation of the TEM-FAST system to Mars exploration.

3. Surface Nuclear Magnetic Resonance (SNMR)

[15] SNMR for detection of subsurface water was first conceived by Varian [1962] but was not implemented until 1978 by the Novosibirsk Institute of Chemical Kinetics and Combustion in the former Soviet Union [Semenov *et al.*, 1982]. Goldman *et al.* [1994] applied SNMR in Israel and major campaigns in the United States to assess the method were undertaken by Lieblich *et al.* [1994] and Hendrickx *et al.* [1999].

[16] In general, NMR exploits the fact that most stable nuclei possess a quantized angular momentum or spin which results in a magnetic moment (see Walstedt [1990] and Goldman *et al.* [1994] for reviews). When an external magnetic field is applied to such nuclei, a weak paramagnetism develops due to the preferential alignment of nuclear moments with the field. This magnetic polarization is too small to be measured directly, but the response of nuclear magnetic moments to a perturbation can be observed. Because most of the magnetic moments lie at some angle to the applied field, they experience a torque that causes them to precess at the Larmor frequency $f_L = \gamma B_o / 2\pi$, where γ is the gyromagnetic ratio and B_o is the applied magnetic induction (Figure 2a). For protons in liquid water, $\gamma = 4.258 \times 10^{-2}$ Hz/nT. A Larmor-frequency field applied at right angles to the static field will cause magnetic moments to nutate or tip away from the static field. In pulsed NMR, the synchronous rotation of magnetic moments is detected in the receiver after the perturbing field is extinguished. The tipping angle is given by

$$\theta = \gamma B_{\perp} t_p \quad (4)$$

where B_{\perp} is the component of the time-varying field that is perpendicular to the static field and t_p is the duration of the pulse. The maximum signal is recorded when nuclei are tipped to 90° from the reference field, a so-called “ $\pi/2$ pulse.” For a current I used to form the pulse, equation (4)

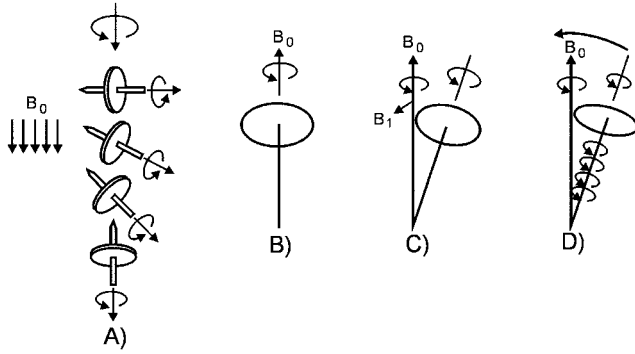


Figure 2a. Schematic illustration of nuclear magnetic resonance (NMR) (after *Hendrickx et al.* [1999]). (a) Spinning nucleus has a magnetic moment, which aligns on average with external field B_0 . (b) Torque causes moments to precess at Larmor frequency. (c) External field applied B_1 applied at right angles to B_0 causes moments to nutate or tip away from B_1 . (d) Moments relax or decay back to equilibrium when B_1 is removed.

may be equivalently written $\theta = Gq$ [*Hendrickx et al.*, 1999] where G is a geometrical factor (see equation (5) below) and $q = It_p$ is the pulse moment.

[17] The return of magnetic moments to equilibrium results in an exponential damping of the sinusoidal NMR signal called free-induction decay (Figure 2b). In geological contexts the decay time constant T_2^* is controlled principally by the ratio of solid surface to liquid volume, i.e., as pore size: $T_2^* \ll 30$ ms for clays but $T_2^* > 300$ ms for gravels [*Schirov et al.*, 1991]. In reality, a distribution of pore sizes requires a spectrum of T_2^* to describe the free-induction decay [e.g., *Kleinberg et al.*, 1994; *Lieblich et al.*, 1994]. Paramagnetic ions in the groundwater will shorten relaxation times; for example, magnetite doping is used to effectively eliminate the response of borehole fluid in downhole NMR [*Ellis*, 1987].

[18] The amplitude of the NMR signal is also attenuated by conductive ground: *Shushakov* [1996] found that resistivity (the reciprocal of conductivity) must be less than a few tens of ohm-meters for this effect to be significant. This occurs where the skin depth is comparable to the aquifer thickness, so the inferred range of resistivity where SNMR attenuation is important must be revised under conditions of different static-field strength (see below).

[19] The most serious geological impediment to SNMR is the presence of magnetic minerals, particularly magnetite [*Hendrickx et al.*, 1999]. The shortening of free-induction decay time was mentioned above. However, the largest effects are due to local magnetic fields: a different static-field magnitude will cause shifts in the Larmor frequency that may be difficult to track, and different static-field directions will change the interaction geometry with the time-varying perturbation field, invalidating the assumptions used to reconstruct water abundance.

[20] The unique features of SNMR compared with its laboratory counterparts lie in the experimental geometry. The pattern of the Larmor-frequency perturbing field from the transmitter loop varies strongly with position; in particular the locus of positions where the perturbing field is

perpendicular to the static field is a function of depth, which allows soundings to be performed. The SNMR signal at transmitter turn-off for a coincident-loop configuration can be calculated from the tipping angle (equation (4)) on an elemental volume of water and the resulting EMF produced back in the loop computed and integrated over the total volume of water as [*Goldman et al.*, 1994]:

$$V^{SNMR} = \omega_L M \int \beta_{\perp} \varphi \sin(\frac{1}{2} \lambda \beta_{\perp} q) dV \quad (5)$$

where $\omega_L = 2\pi f_L$ is the angular Larmor frequency, $M = 1.92 \times 10^{-7}$ J/(T-m³) is the proton magnetization or equilibrium magnetic moment, φ is the porosity (here assumed saturated), $\beta_{\perp} = B_{\perp}/I_p$ is the specific induction vector or perpendicular component of the perturbing field normalized by transmitter current, and q is the pulse moment given above. Note that a multiturn coil will increase q by the number of turns. The factor of 1/2 arises because the linear polarization of the transmitted field may be decomposed into two counter-rotating circular polarizations, only one of which contributes to the resonance. Also note that the pulse duration must be rather less than the decay-time constant $t_p \ll T_2^*$ for equation (5) to hold.

[21] The direct proportionality of ω_L and V^{SNMR} is a consequence of measuring EMF. The average vertical magnetic field within the loop can be easily derived from the integral form of Faraday's Law $B_z^{SNMR} \approx (-1/nD^2) \int V^{SNMR} dt = -V^{SNMR}/nD^2\omega_L$. The magnetic field of the resonating nuclei is independent of the Larmor frequency of the excitation.

[22] Evaluation of equation (5) for 10-m thick aquifers with 10% porosity at depths of 10, 30, and 50 m illustrates the principal features of the SNMR response as typically observed in terrestrial exploration (Figure 3). The 100-m diameter, 1 A, single-turn transmitter loop is considered to be square for computational simplicity [*Das et al.*, 1990]. The static field is 50,000 nT and has an inclination of 45°. The Larmor frequency is 2130 Hz, a typical value. For the shallowest aquifer, the maximum response is observed at $q =$

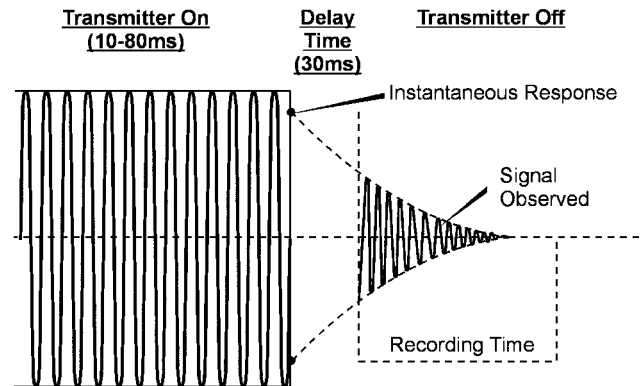


Figure 2b. Time series for pulsed NMR (after *Hendrickx et al.* [1999]). Nuclei rotate synchronously with magnetic field applied at Larmor frequency during transmitter on-time. After transmitter turn-off, signal follows free-induction decay with one or more time constants characteristic of formation porosity. Switching delay can likely be substantially reduced in next-generation equipment.

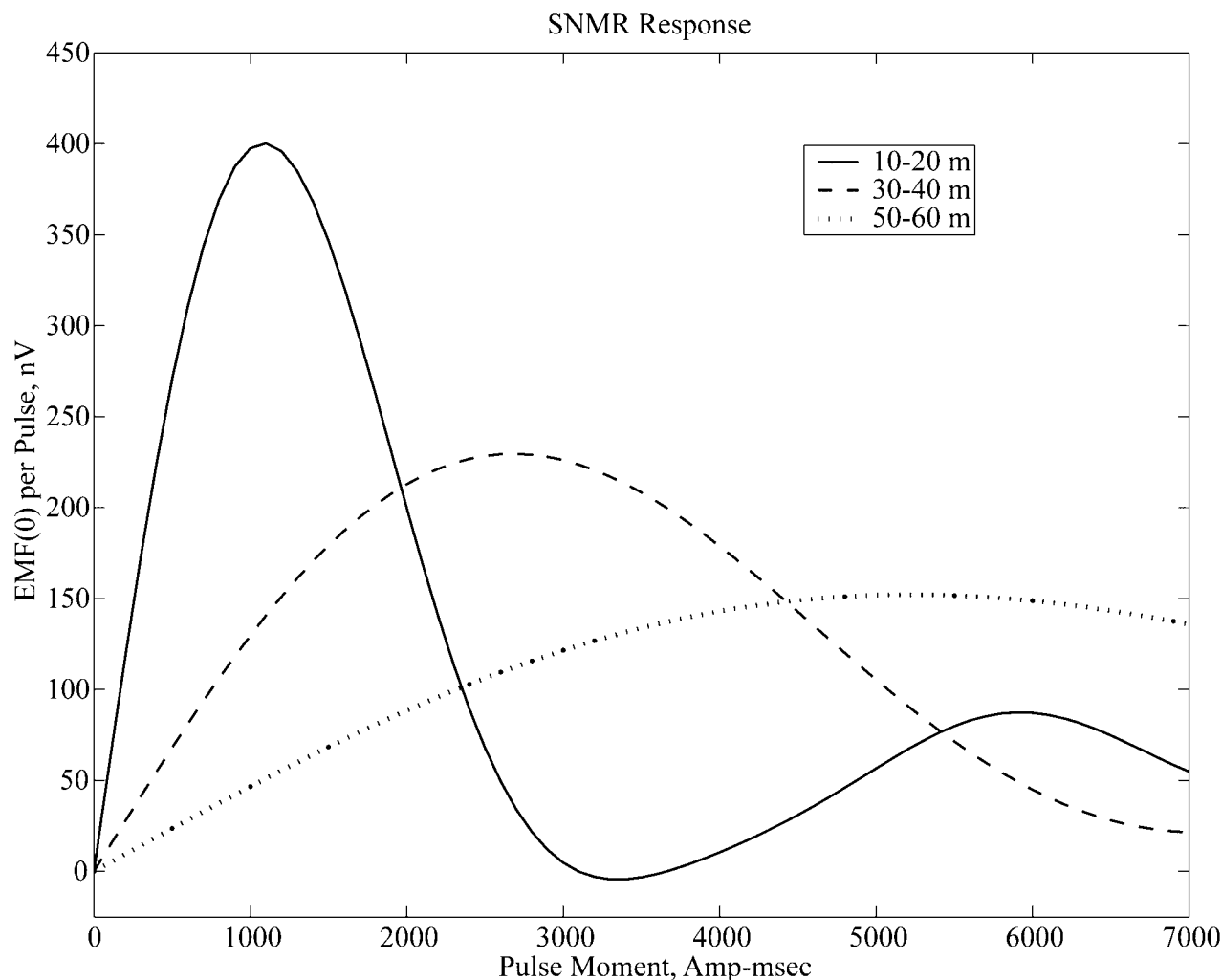


Figure 3. Calculated surface nuclear magnetic resonance (SNMR) response for 10% porosity, saturated aquifer with fixed 10-m thickness at three different depths (see text for other parameters). Maximum response occurs when protons beneath loop are tipped to 90° , 270° , etc. Reduced amplitude at higher pulse moment is due to destructive interference of increasingly tipped protons in more distant parts of the aquifer, and broader responses are due to spin tipping of a relatively larger part of deeper targets.

1100 A-ms, which corresponds to an average $\pi/2$ pulse into part of the aquifer nearly beneath the coil. At greater pulse moments, the hydrogen nuclei are tipped greater than 90° and so the signal is smaller, leading to a minimum 180° -response at $q = 3300$ A-ms. Still increasing the pulse moment, a second peak is reached at $q = 5900$ A-ms, but the amplitude is smaller because hydrogen nuclei in more distant parts of the aquifer are experiencing sufficient tipping to interfere with the 270° rotations of the near-transmitter portions. Where the aquifer is deeper, the maximum NMR signal is smaller and the pulse moment for $\pi/2$ tipping is larger because of the reduced amplitude of the perturbing field and the reciprocal falloff back to the receiver. The pulse-moment distribution is broader because a larger part of the target is affected at depth. Note that where the tipping angle is small and $\sin \theta \approx \theta$ in equation (5), the response varies linearly with pulse moment.

[23] The Russian SNMR has been commercialized by Iris Instruments, Inc. as the NUMIS system (www.iris-instruments.com) and consists of (1) a 70-kg power supply, (2) a 40-kg power converter, (3) two 24-V car batteries, (4) a laptop PC, and (5) a user-specified circumference of 25-mm diameter wire for the transmitter/receiver loop. For a 100-m diameter loop the wire mass is 140 kg, bringing the total mass of the system to 250 kg. This is a large mass even by EM standards but is necessary to sustain pulse moments of thousands of A-ms using I_p up to 300 A at $t_p \sim 30$ ms. The stated receiver noise density is 10 nV/ $\sqrt{\text{Hz}}$.

iris-instruments.com) and consists of (1) a 70-kg power supply, (2) a 40-kg power converter, (3) two 24-V car batteries, (4) a laptop PC, and (5) a user-specified circumference of 25-mm diameter wire for the transmitter/receiver loop. For a 100-m diameter loop the wire mass is 140 kg, bringing the total mass of the system to 250 kg. This is a large mass even by EM standards but is necessary to sustain pulse moments of thousands of A-ms using I_p up to 300 A at $t_p \sim 30$ ms. The stated receiver noise density is 10 nV/ $\sqrt{\text{Hz}}$.

4. Application to Mars

[24] The high cost per unit mass of landed assets on the surface of Mars requires that sounding systems should be as lightweight as possible and that the same system should double as SNMR and TDEM. To illustrate the comparative performance of SNMR and TDEM under these conditions, first assume that the mass of the transmitter loop is just 1 kg but that this mass can be distributed as a single-turn, 100-m

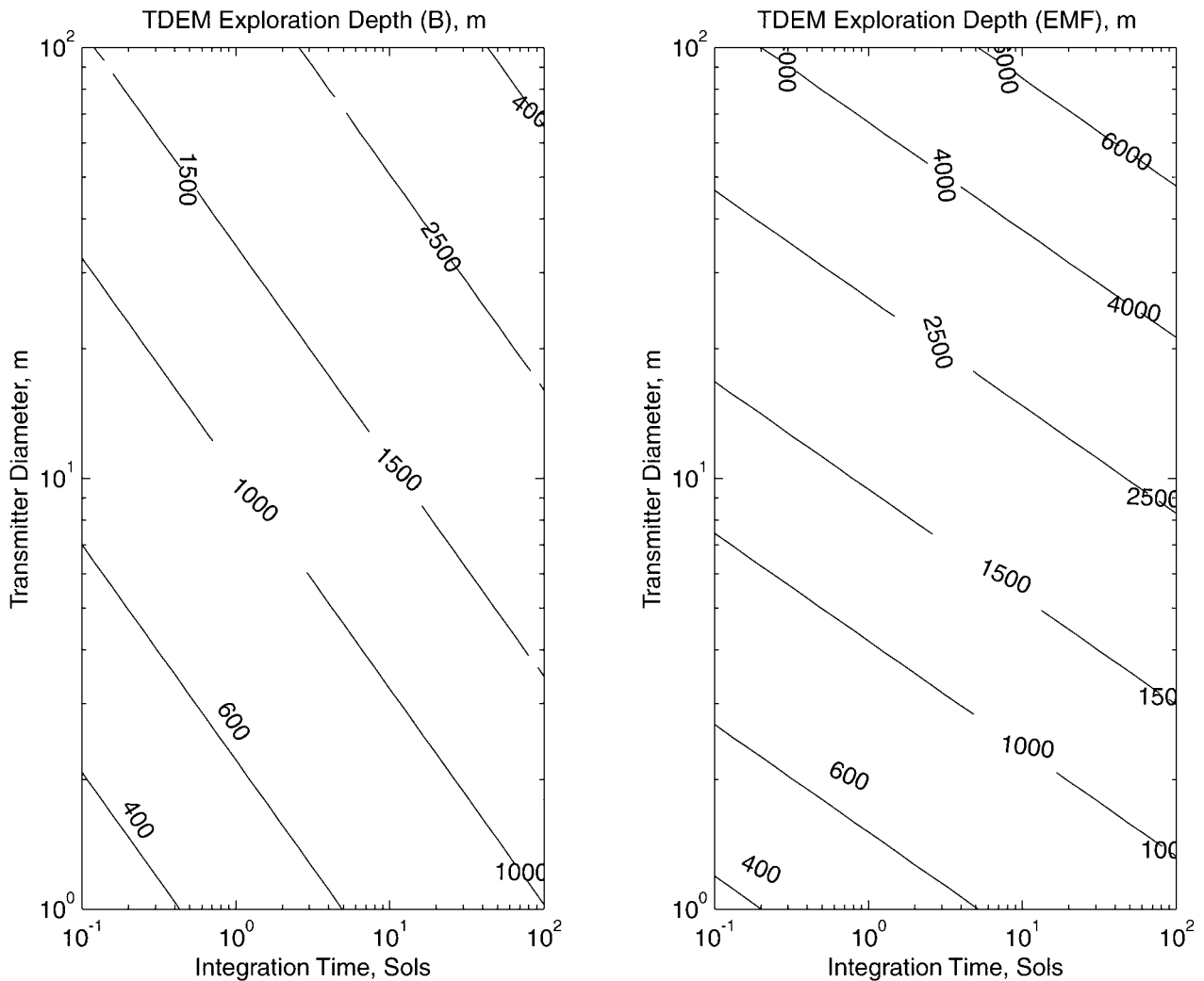


Figure 4. TDEM exploration depth for aquifers on Mars, modeled as thin conductive plates, as functions of integration time and transmitter diameter. EMF (left) is assumed to be measured in coincident-loop mode, whereas magnetic field (right) is measured using a separate receiver. See text for other parameters. Useful integration time will in practice be limited by noise stationarity. Even for short integration times, water can be detected to depths of at least several hundred meters.

loop or as a multiturn, smaller loop. For purposes of visual presentation, nonintegral numbers of turns will be allowed to prevent discontinuities from appearing in the plots at low numbers of turns. A 1-kg, 21-gauge (0.7-mm diameter) copper transmitter wire will dissipate 5 W at 50% duty.

[25] Next assume that sufficient separation between the receiver and lander can be achieved so that radiated and eddy-current electromagnetic interference (EMI) are negligible. Then the noise density is determined by the environment and/or the receiver system self-noise (note that power line noise is the largest single source of measurement error in terrestrial SNMR). For EMF measurements a noise density of 30 nV/ $\sqrt{\text{Hz}}$ was assigned as representative of the geometric mean among several different EM receiver units. For magnetic field measurements a noise density of 0.1 pT/ $\sqrt{\text{Hz}}$ was selected to be the geometric mean among values representative of large receiver coils of several kilogram mass and compact coils or magnetometers of tens or hundreds of grams. For comparison a typical terrestrial

magnetic field noise level from all sources is ~ 1 pT/ $\sqrt{\text{Hz}}$ [Spies and Frischknecht, 1991].

[26] In both the TDEM and SNMR models presented here, the resistivity of the overburden is assumed to be infinite. The porosity of the saturated aquifer is taken to be 10% and the formation water is considered to be in equilibrium with moderate clay abundance, resulting in a net resistivity of 100 $\Omega\text{-m}$ [see Grimm, 2002]. This value is typical of the near surface of the Earth. The plate thickness is fixed at 100 m, representing either a discrete layer of water or an aquifer above an semi-infinite, saturated aquitard whose pore size is too small to yield a measurable SNMR response.

[27] Magnetic fields measured by MGS exceed 1000 nT at 100–200 km altitude for portions of Mars [Acuña *et al.*, 1999]. However, the fields at the surface of Mars are unknown and cannot be fully reconstructed from orbital measurements because the short wavelengths are completely attenuated. Arguing solely by analogy, magnetic

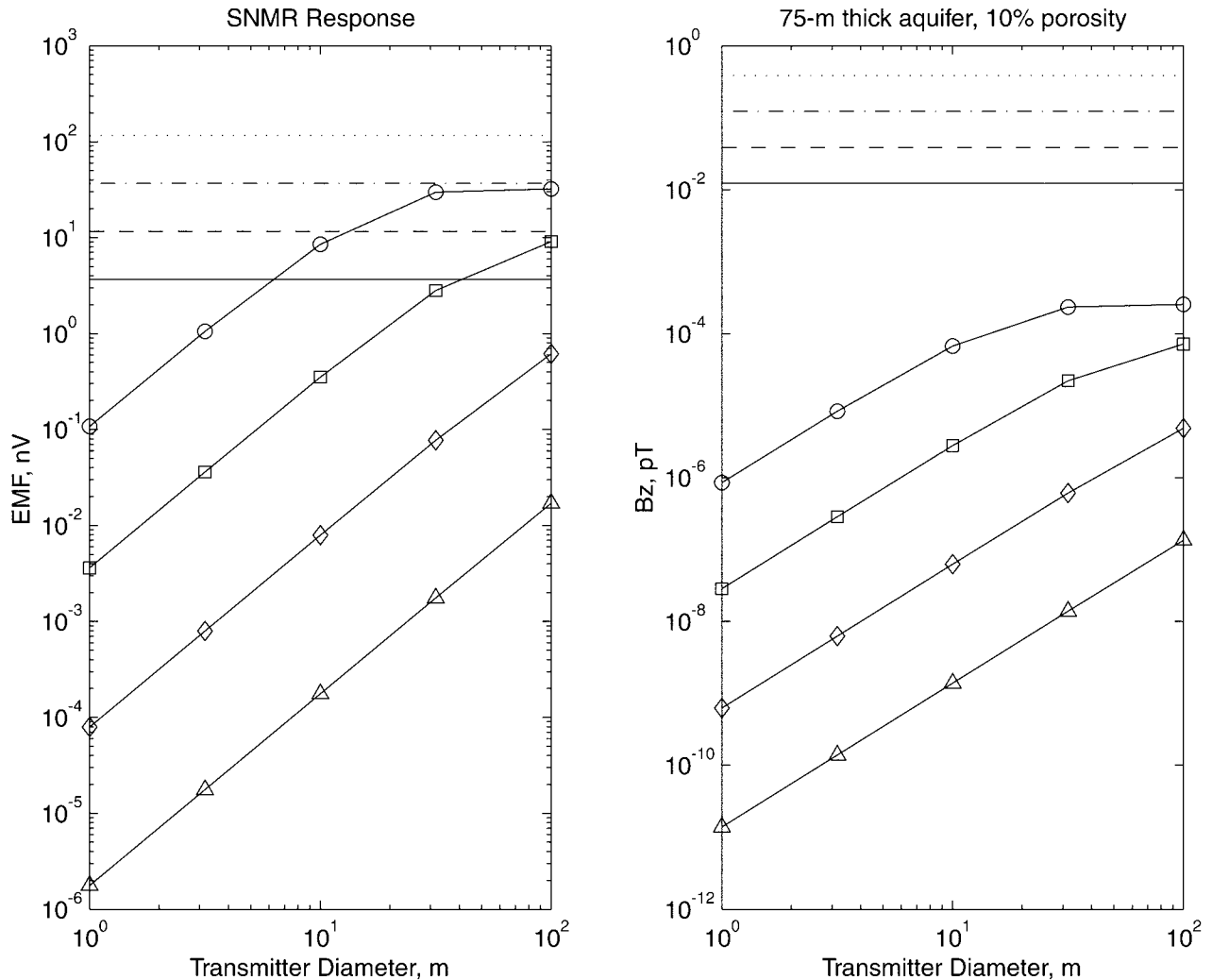


Figure 5. SNMR response for the same transmitter/receiver and aquifer characteristics as used for TDEM, assuming Earth-like static magnetic field. The signal per pulse for different aquifer depths is plotted against the effective noise level after stacking and SNR requirement. Aquifers are at depths of 10 m (circles), 30 m (squares), 100 m (diamonds) and 300 m (triangles). Horizontal lines show noise levels after integration times of 0.1 sols (dot), 1 sol (dash-dot), and 10 sols (dash), and 100 sols (solid); again, note that effective integration time is limited by noise stationarity. With the resources specified, SNMR measuring EMF can detect water only to depths of tens of meters and only with relatively large transmitter loops and stacking times. Magnetic fields are too small to be detected.

fields that arise in the terrestrial lithosphere are tens of nanoTeslas at altitudes comparable to MGS, suggesting that fields over at least some of the surface of Mars could be 10–100X those of Earth. The static-field strength will be treated here simply as a free parameter, with the Larmor frequency increasing proportionally. However, the depth of penetration of the time-varying field into the aquifer is limited by the skin depth, $\approx 500 \sqrt{\rho/f_L}$ in meters, where ρ is the resistivity. *Shushakov* [1996] developed a formal solution for SNMR in conductive ground. For the simple conductive-plate model used here a commensurately simple estimate can be used. The depth of exploration of inductive methods is commonly taken to be $\sim 7/10$ of a skin depth, i.e., to the depth at which the signal decreases by half [e.g., *McNeill*, 1990]. As a first approximation the portion of the plate above this cutoff will be assumed to provide the full

SNMR response and the deeper portion neglected. At 2 kHz, the cutoff depths for 100, 10, and 1 Ω -m are approximately 75, 25, and 10 m, respectively, consistent with the results of *Shushakov* [1996]. For fields 10X and 100X those of Earth, the higher Larmor frequencies yield cutoff depths for a 100 Ω -m aquifer of 25 and 10 m, respectively.

[28] A required signal-to-noise ratio of 10 is enforced for both systems. The pulse rate f_T and sampling-gate width Δ for TDEM were selected to be 200 s^{-1} and 0.1 ms, respectively, so that both the initial amplitude and falloff could be adequately tracked for this particular aquifer conductance [see *Grimm*, 2002]. The SNMR pulse duration is $t_p = 30$ ms, which is short enough to observe free-induction decay even in fine-grained aquifers [see *Schirov et al.*, 1991]. The pulse rate for the NUMIS system is only 0.125 s^{-1} but here it is assumed that 1 s^{-1} can be

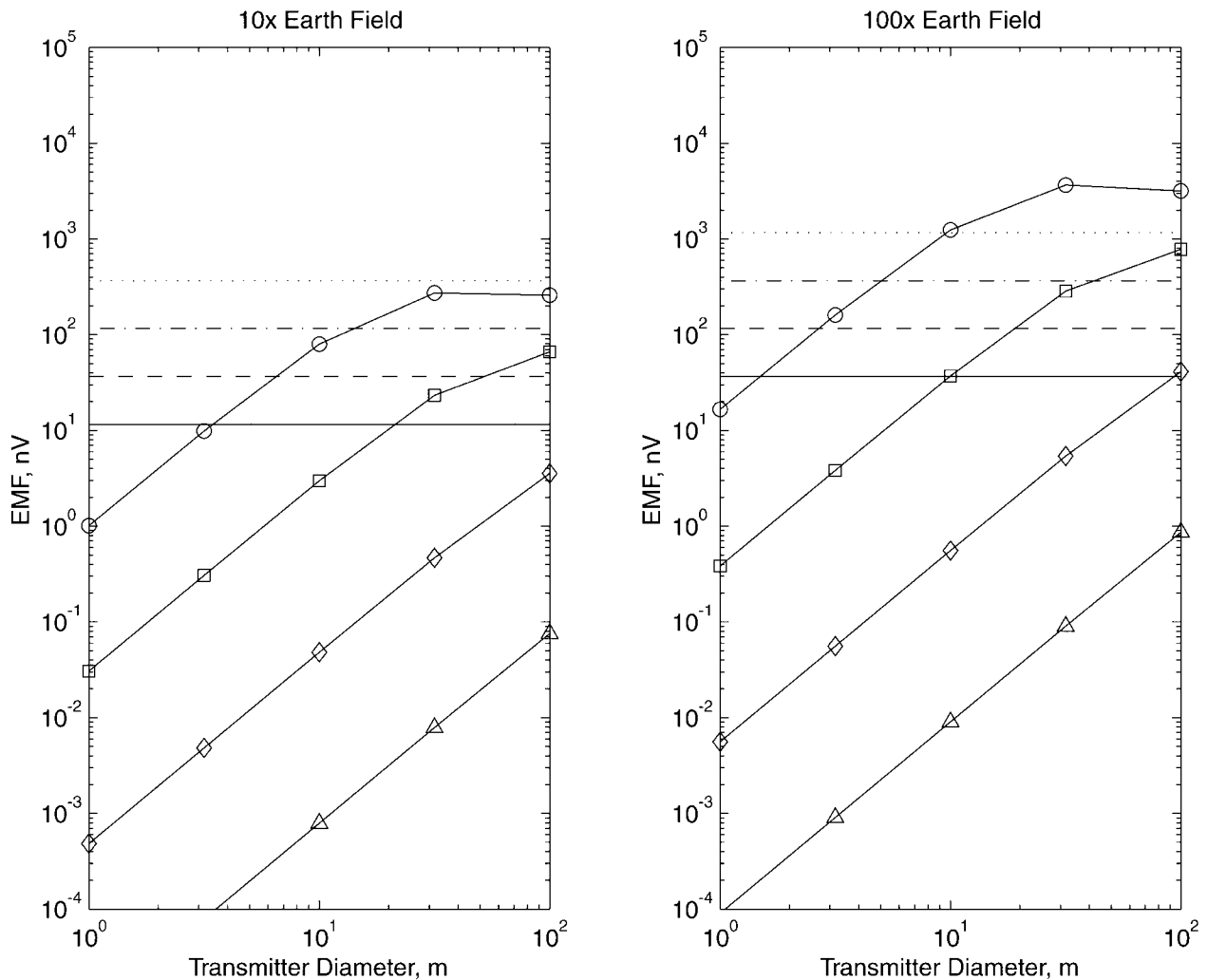


Figure 6. As Figure 5, but for static magnetic fields 10X (left) and 100X (right) of Earth's average field. Results are approximately corrected for decreasing penetration into aquifer at higher Larmor frequencies by modeling aquifer thicknesses equal to 7/10 of skin depth, or 25 m (left) and 10 m (right). There is no improvement in signal-to-noise ratio beyond the 100X field due to skin-depth limitations. Only EMF response is shown as magnetic fields are still below detection thresholds.

accommodated, which should allow for three characteristic decay times (95% of amplitude) even for coarse-grained sediments [see *Schirov et al.*, 1991]. The sampling-gate width is set to the maximum allowed, the Nyquist rate for f_L . The static magnetic field is assumed initially to be 50,000 nT (i.e., Earth-like) with an inclination of 45° ; results are not very sensitive to the latter.

[29] The exploration depth of the small TDEM system is clearly sufficient to detect water at depths of hundreds of meters for small loops and relatively short integration times (Figure 4). Using large loops, water could be detectable to depths of several kilometers if the noise is stationary such that longer integrations were stable. For the aquifer and sensor characteristics selected here, EMF measurements are more efficient than magnetic field measurements. Note from equations (1) and (2) that the exploration depths scale as transmitter current to the one-third power when measuring magnetic field and as transmitter current to the one-fourth power when measuring EMF. Therefore doubling the explo-

ration depths plotted can be achieved by an order-of-magnitude increase in the transmitter current I or in the number of turns n on the transmitter loop; either would imply an order-of-magnitude increase in system mass. For a coincident-loop system measuring EMF, the exploration depth increases as \sqrt{n} . Diminishing returns would argue against such increases when searching for shallow water, but if deep aquifers are to be completely characterized, a larger system may be necessary [see *Grimm*, 2002].

[30] In contrast, the exploration depth of SNMR using the same resources is very limited (Figure 5). Under a terrestrial-strength static field, the maximum depth to which the specified aquifer can be detected is ~ 30 m, using a 100-m loop and signal-integrating for 10 sols. Aquifers at 100-m would require ~ 1000 sols of stacking even for this large loop. These results are for EMF measurements; the SNMR magnetic fields are so small they cannot be detected at all. The increase in signal with loop size, in spite of the fact that higher pulse moments exist for the smaller, multiturn coils,

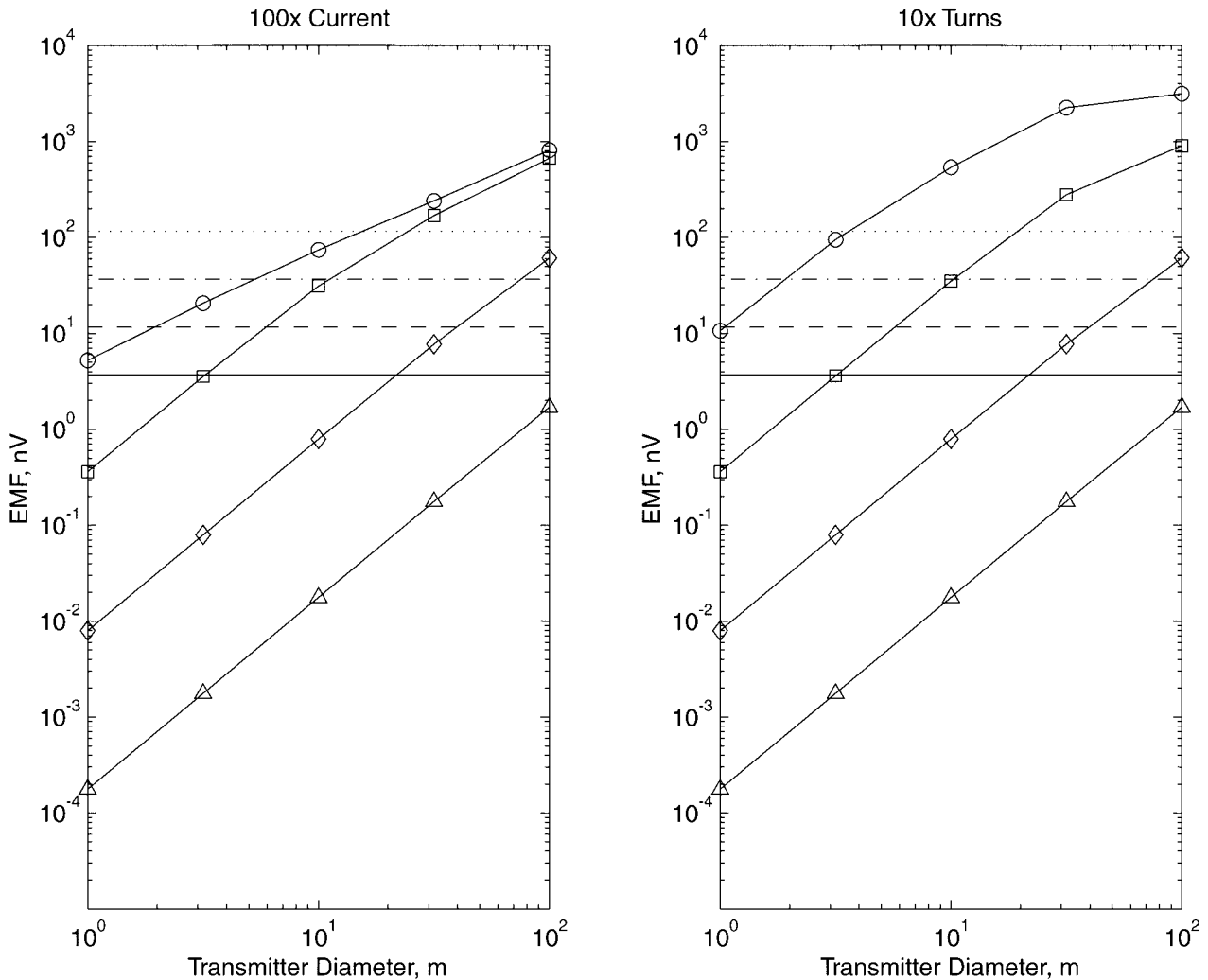


Figure 7. As Figure 5, but for 100X current (left) or 10X loop turns (right). The latter is more efficient as the EMF is proportional to both the increased effective transmitter current and the increased effective receiver area. Detection of water at hundreds of meters depth is still difficult in both cases.

indicates that the volume of the aquifer “illuminated” is more important the pulse moment. The departure from a power law for the largest loops and shallowest aquifers is a consequence of the nonlinearity where $\sin \theta \approx \theta$ no longer applies and a significant volume of protons are being tipped through 90° .

[31] Regions of higher static magnetic field would be associated with a proportionally higher Larmor frequency and hence higher a proportionally EMF response. Two other factors largely negate this improvement, however. First, the noise bandwidth is also proportional to the Larmor frequency because a higher sampling rate must be used: this reduces the SNR improvement to a factor of just $\sqrt{f_L}$. Second, the depth to which the aquifer is probed is controlled by the skin depth, which is inversely proportional to $\sqrt{f_L}$. In the limit, there is no increase in SNR with increasing Larmor frequency when sensing of the target is fully skin-depth limited. For the model presented here, this limit is reached for static-field strengths about 100 times that of Earth (Figure 6). Even so, exploration depths are still generally limited to tens of meters; a 100-m deep target

could be detected only after 1000 sols of integration using a 100-m loop.

[32] Higher transmitter current or increasing the number of loop-turns appears to be the only reasonable way to boost the SNMR signal (Figure 7). A hundredfold increase in current results in a proportional increase in the signal of aquifers at depths of 100 m or more, but detection is still marginal and the power supplies for such large currents would require tens of kilograms or greater, even allowing for an order-of-magnitude decrease in the mass of present commercial systems. Increasing the number of turns on the loop is a technically simpler and more cost-effective approach, as the EMF increases as the square of n . It is still apparent from Figure 7, however, that further increases in the number of turns and/or current is necessary to detect water at depths of hundreds of meters.

5. Concluding Discussion

[33] The models presented here show that for identical resources and an Earth-like static magnetic field, the explo-

ration depth of SNMR is one to two orders of magnitude smaller than TDEM. In order to improve the SNMR exploration depth to hundreds of meters, the minimum necessary to search for “shallow” groundwater on Mars, system masses of tens to hundreds of kilograms in the form of large transmitters (for high current) or multiturn loops (providing both current and EMF multipliers) are necessary. The latter will be increasingly hard to turn off abruptly due to self-inductance. Regions of strong crustal magnetism on Mars will provide a proportional boost in SNR only until the skin-depth limit is reached. Superparamagnetic ground responses could obliterate any signal in coincident-loop measurements, so extra mass must be budgeted to carry a multiturn receiver coil ($\sim 10^4$ m², comparable to the large loops) and its deployment mechanism.

[34] The models presented here assume that both TDEM and SNMR will simply begin measurements and continue to stack in signal until the detection threshold is reached. In practice, both methods require a search for the optimum frequency. In TDEM the pulse period must be selected so that both early and late times in the decay can be resolved, whereas in SNMR the resonant Larmor frequency must be sought. Because of the strong variability in magnetic fields at the surface of Mars, the Larmor frequency may be difficult to find. Furthermore, randomly oriented magnetic particles in an impact regolith will further attenuate the SNMR signal.

[35] The unambiguous detection of groundwater on Mars by SNMR is unlikely to be achieved without massive resources, perhaps those that must await human exploration. Classical low-frequency EM methods provide robotic reconnaissance missions the best trade of sensitivity to water (with some nonuniqueness) versus system size, mass, and power.

[36] NASA’s recently proposed Prometheus Project might provide nuclear power sources that could extend the depth of both TDEM and SNMR soundings. Also, the adopted EMF noise density was for a fixed transmitter-loop area; the relative changes in signal-to-noise for different areas are the same for TDEM and SNMR.

[37] **Acknowledgments.** I thank Mark Blohm for helpful discussions. This work was supported by the NASA Mars Program Office under a Mars Scout Concept Study contract.

References

- Acuña, M., et al., Global distribution of crustal magnetization discovered by the Mars Global Surveyor MAG/ER experiment, *Science*, 284, 790–793, 1999.
- Becker, A., and G. Cheng, Detection of repetitive electromagnetic signals, in *Electromagnetic Methods in Applied Geophysics*, vol. 1, *Theory*, edited by M. N. Nabighian, pp. 443–466, Soc. Explor. Geophys., Tulsa, Okla., 1988.
- Blacic, J. D., D. S. Dreesen, and T. Mockler, *Report on Conceptual Systems Analysis of Drilling Systems for 200-m Depth Penetration and Sampling of the Martian Subsurface*, Los Alamos Natl. Lab., Los Alamos, N.M., 2000. (available at www.ees4.lanl.gov/mars)
- Christensen, P. R., et al., Detection of crystalline hematite mineralization on Mars by the Thermal Emission Spectrometer: Evidence for near-surface water, *J. Geophys. Res.*, 105, 9623–9642, 2000.
- Clifford, S. M., A model for the hydrologic and climatic behavior of water on Mars, *J. Geophys. Res.*, 98, 10,973–11,065, 1993.
- Das, Y., J. E. McFee, J. Toews, and G. C. Stuart, Analysis of an electromagnetic induction detector for real-time location of buried objects, *IEEE Trans Geosci. Rem. Sens.*, 28, 278–287, 1990.
- Ellis, D. V., *Well Logging for Earth Scientists*, Elsevier Sci., New York, 1987.
- Goldman, M., B. Rabinovich, M. Rabinovich, D. Gilad, I. Gev, and M. Schirov, Application of the integrated NMR-TDEM method in groundwater exploration in Israel, *J. Appl. Geophys.*, 31, 27–52, 1994.
- Grimm, R. E., Low-frequency electromagnetic exploration for groundwater on Mars, *J. Geophys. Res.*, 107(E2), 5006, doi:10.1029.2001JE001504, 2002.
- Hendrickx, J., T. Yao, A. Kearns, P. Hoekstra, R. Blohm, M. Blohm, P. Weichman, and E. Lavelly, Nuclear magnetic resonance imaging of water content in the subsurface, *Cont. DE-FG07-96ER14732*, Off. of Energy Res., U.S. Dept. of Energy, Washington, D. C., 1999.
- Hoekstra, P., and M. W. Blohm, Case histories of time-domain electromagnetic soundings in environmental geophysics, in *Geotechnical and Environmental Geophysics*, vol. 2, *Environmental and Groundwater*, edited by S. H. Ward, pp. 1–16, Soc. Explor. Geophys., Tulsa, Okla., 1990.
- Kaufman, A. A., *Geophysical Field Theory and Method*, part C, *Electromagnetic Fields II*, 332 pp., Academic, San Diego, Calif., 1994.
- Kleinberg, R. L., W. E. Kenyon, and P. P. Mitra, Mechanism of NMR relaxation of fluids in rock, *J. Magn. Reson., Ser. A*, 108, 206–214, 1994.
- Lieblich, D. A., A. Legchenko, F. P. Haeni, and A. Portselan, Surface nuclear magnetic resonance experiments to detect subsurface water at Haddam Meadows, Connecticut, *Symp. Appl. Geophys. Eng. Environ. Problems (SAGEEP)*, 94, 717–736, 1994.
- Malin, M. C., and K. S. Edgett, Evidence for recent groundwater seepage and surface runoff on Mars, *Science*, 288, 2330–2335, 2000.
- Mars Exploration Program/Payload Analysis Group (MEPAG), *Science Planning for Exploring Mars*, part 2, *Scientific Goals, Objectives, and Priorities*, edited by R. Greeley, Jet Propulsion Lab., Pasadena, Calif., 2001.
- McNeill, J. D., Use of electromagnetic methods for groundwater studies, in *Geotechnical and Environmental Geophysics*, vol. 1, *Review and Tutorial*, edited by S. H. Ward, pp. 191–218, Soc. Explor. Geophys., Tulsa, Okla., 1990.
- Muhleman, D. O., B. J. Butler, A. W. Grossman, and M. A. Slade, Radar images of Mars, *Science*, 253, 1508–1513, 1991.
- Ozorovich, Y. R., V. M. Linkin, and W. D. Smythe, Mars electromagnetic sounding experiment MARSES (abstract 1549), *Lunar Planet. Sci. XXX*, 1999.
- Schirov, M. D., A. V. Legchenko, and J. G. Creer, New direct non-invasive groundwater detection technology for Australia, *Explor. Geophys.*, 22, 333–338, 1991.
- Semenov, A. G., A. Y. Pusep, and M. D. Schirov, *Hydroscope-An Installation for Prospecting Without Drilling* (in Russian), 26 pp., USSR Acad. Sci., Novosibirsk, 1982.
- Shushakov, O., Groundwater NMR in conductive water, *Geophysics*, 61, 988–1006, 1996.
- Spies, B. R., and F. C. Frischknecht, Electromagnetic sounding, in *Electromagnetic Methods in Applied Geophysics*, vol. 2, *Application*, edited by M. N. Nabighian, pp. 285–386, Soc. Explor. Geophys., Tulsa, Okla., 1991.
- Varian, N. H., Ground liquid prospecting method and apparatus, Patent 3,019,383, U.S. Patent and Trademark Off., Washington, D. C., 1962.
- Walstedt, R. E., Nuclear magnetic resonance, in *Encyclopedia of Physics*, 2nd ed., edited by R. G. Lerner and G. L. Trigg, pp. 831–833, John Wiley, New York, 1990.

R. E. Grimm, Blackhawk Geoservices, Inc., 310 B Commercial Road, Golden, CO 80401, USA. (grimm@blackhawkgeo.com)